Linear and cubic dynamic susceptibilities of superparamagnetic fine particles

Yuri L. Raikher and Victor I. Stepanov
Institute of Continuous Media Mechanics, Urals Branch of RAS, 614013, Perm, Russia
(Received 21 February 1997)

A consistent theory of linear and nonlinear (cubic) initial susceptibilities of an assembly of uniaxially anisotropic noninteracting fine magnetic particles is presented. The expressions for the static (equilibrium) susceptibilities are obtained directly from the pertinent statistical thermodynamics. The contributions of anisotropy emerge yet in the first order and are analyzed for random and axes-aligned distributions. The ac susceptibilities are studied on the basis of the micromagnetic Fokker-Planck equation. Both a numerically exact solution for arbitrary frequency and a reliable low-frequency approximation are given. The obtained description proves to be more accurate as compared to the one based on the customary superparamagnetic blocking model. The results are used for a quantitative interpretation of recently published set of data on Co-Cu precipitating alloys. In this connection the choice of the particle size-distribution function is discussed. [S0163-1829(97)04722-X]

INTRODUCTION

Since the very first studies of fine-particle systems,[1] the development of the micromagnetic science was inspired mainly by the necessity to predict the magnetic properties and response of a ferromagnetic particulate media. Beyond argument, in this objective the fundamental and applicational aspects are tied up very closely, if not inseparably.

The problem of prime interest while performing experiments on or manufacturing fine-particle magnetic systems is to characterize the magnetic content of the sample with as few measurements as possible. Magnetic granulometry by means of a quasistatic magnetization curve is very well known and widely used.[1–3] The dynamic approach, where simultaneously linear and nonlinear susceptibilities are taken into account is more new, being most probably inspired by its use in the spin-glass science. To justify the method, one should process a good deal of experimental data with the aid of an appropriate theory. Such a work has been attempted recently in Refs. 4,5 with a precipitating Cu-Co alloy as a test object. The authors had no difficulties in fitting the linear susceptibility measurements with the aid of superparamagnetic blocking model assuming that: (i) the particles are single domain and their magnetization does not depend on temperature, (ii) the magnetic anisotropy is uniaxial and has one and the same value for all the particles, and (iii) the magnetic dipole-dipole interaction is negligible. It was fitting the nonlinear (cubic) susceptibility data where a problem arose, since there was no theory for it insofar, consistent with the aforementioned assumptions. To fill the place, in Refs. 4,5 were employed the formulas originally derived for an *isotropic* superparamagnet. They were adjusted by replacing the pertinent relaxation time with a one exponential in the *magnetic anisotropy* constant K. However, the resulting agreement turned out to be poor. From that the authors of Refs. 4,5 concluded to that some of the basic assumptions (i)–(iii) are wrong. From our viewpoint, in the first place this reproach should be addressed not to the classic superparamagnetic theory as itself but to a rather ''intuitive'' manner of its usage.

The incentive and the main goal of our paper is to consistently extend the conventional theory on the case of a nonlinear response and by that to confirm its validity. While doing that we propose practical schemes (both exact and approximate) to handle linear and cubic dynamic responses in the framework of classical superparamagnetism. Applying our results to the reported data on the nonlinear susceptibility of Cu-Co precipitates, we demonstrate that a fairly good agreement may be achieved easily.

I. STATIC SUSCEPTIBILITIES

As a starting point we take an isolated single-domain particle of a ferro- or ferrimagnetic material rigidly trapped in the bulk of a solid nonmagnetic matrix. Single domain has a spatial uniformity of the spin alignment over the grain that enables us to describe it by the net magnetic moment $\boldsymbol{\mu}=\mu\boldsymbol{e}$, whose direction is given by a unit vector $\boldsymbol{e}$. The magnetic moment magnitude is $\mu=Iv$ with I the saturation magnetization of the material at given temperature and v being the particle volume. Besides that, we assume the particle to possess a uniaxial magnetic anisotropy with an energy density K and a direction defined by a unit vector $\boldsymbol{n}$.

If the external magnetic field $\boldsymbol{H}$ is not too high as to affect the atomic magnetic structure, its only effect on a single-domain grain is the magnetic moment rotation. Then the corresponding orientation-dependent part of the particle energy U may be written as

$$U=-Kv(\boldsymbol{en})^2-\mu(\boldsymbol{eH}). \tag{1}$$

The stationary distribution function of the particle magnetic moment or (if we neglect interactions) of an assembly of magnetic moments is determined by the Gibbs formula

$$W(\boldsymbol{e})=Z^{-1}\exp(\sigma(\boldsymbol{en})^2+\xi(\boldsymbol{eh})),$$

$$Z(\sigma,\xi)=\int \exp(\sigma(\boldsymbol{en})^2+\xi(\boldsymbol{eh}))d\boldsymbol{e}, \tag{2}$$

where

$$\sigma = Kv/k_BT, \quad \xi = \mu H/k_BT, \tag{3}$$

and $\boldsymbol{h}$ is a unit vector along the external magnetic field.

In what follows we shall consider a situation where the external magnetic field is weak enough, and does not too strongly change the basic state of the system. Assuming the value of ξ to be small, one gets by expanding Eq. (2)

$$W(\boldsymbol{e}) = W_0 \frac{1 + \xi(\boldsymbol{eh}) + \frac{1}{2}\xi^2(\boldsymbol{eh})^2 + \frac{1}{6}\xi^3(\boldsymbol{eh})^3}{1 + \frac{1}{2}\xi^2\langle(\boldsymbol{eh})^2\rangle_0}, \tag{4}$$

where the distribution and partition functions

$$W_0(y) = Z_0^{-1}\exp(\sigma y^2), \quad Z_0(\sigma) = 2\pi\int_{-1}^{1}\exp(\sigma y^2),$$

$$y = (\boldsymbol{en}), \tag{5}$$

describe the unperturbed state $\boldsymbol{H}=0$. Accordingly, the angular brackets with a subscript 0 in Eq. (4) designate averaging with respect to the distribution (5).

Due to evenness of W_0, all the odd moments of the equilibrium distribution (5) vanish. In particular, it means zero net magnetization. The latter may appear only as a response to an applied field. Assuming that the interparticle interaction may be neglected, one finds that $M/c\mu$, the reduced magnetization in the direction of the field, equals the mean cosine $\langle(\boldsymbol{eh})\rangle$. With the distribution (4) it reads

$$M/c\mu = \langle(\boldsymbol{eh})\rangle = \langle(\boldsymbol{eh})^2\rangle_0\xi + [\tfrac{1}{6}\langle(\boldsymbol{eh})^4\rangle_0 - \tfrac{1}{2}\langle(\boldsymbol{eh})^2\rangle_0^2]\xi^3, \tag{6}$$

where c is the particle number concentration.

To evaluate the averages like those in Eq. (6), it is very convenient to pass from cosines $\langle(\boldsymbol{en})^k\rangle$ to the set of corresponding Legendre polynomials for which a spherical harmonics expansion (addition theorem)

$$P_l(\boldsymbol{eh}) = \frac{4\pi}{2l+1}\sum_{m=-l}^{l} Y_{lm}^*(\boldsymbol{nh})Y_{lm}(\boldsymbol{en}), \tag{7}$$

takes place.

Taking into account a uniaxial symmetry of the distribution function W_0, upon averaging of Eq. (7) one gets a generic formula

$$\langle P_l(\boldsymbol{eh})\rangle_0 = S_l P_l(\boldsymbol{nh}), \quad \text{for } l \text{ even};$$

$$\langle P_l(\boldsymbol{eh})\rangle_0 = 0, \quad \text{for } l \text{ odd}; \tag{8}$$

where

$$S_l(\sigma) = \langle P_l(\boldsymbol{en})\rangle_0 = \int_{-1}^{1} P_l(y)W_0(y)dy. \tag{9}$$

The order parameters grow from zero with σ and saturate at the unity value. The corresponding asymptotic relations read

$$S_l(\sigma) = \begin{cases} \dfrac{(l-1)!!}{(2l+1)!!}\sigma^{l/2} + \ldots & \text{for } \sigma \ll 1, \\ 1 - \dfrac{l(l+1)}{4\sigma} + \ldots & \text{for } \sigma \gg 1. \end{cases} \tag{10}$$

We remark that the first term of this set, S_2, has the meaning of the internal orientational magnetic order parameter, and as such coincides with the normalized Edwards-Anderson parameter q which is in use in the spin-glass theory. The main difference is that in a spin glass it is caused by the exchange interaction while here, by the magnetic anisotropy energy, i.e., either spin-orbit or spin dipole-dipole coupling.

With the introduced notations, the dimensionless magnetization (6) transforms into

$$\langle(\boldsymbol{eh})\rangle = \frac{1 + 2S_2P_2(\boldsymbol{nh})}{3}\xi - \frac{7 + 70[S_2P_2(\boldsymbol{nh})]^2 + 40S_2P_2(\boldsymbol{nh}) - 12S_4P_4(\boldsymbol{nh})}{315}\xi^3. \tag{11}$$

Comparison of Eqs. (6) and (11) with the standard definition of the magnetic response

$$M = \chi^{(1)}H + \chi^{(3)}H^3 + \chi^{(5)}H^5 + \cdots, \tag{12}$$

yields explicit expressions for the first two terms: linear ($\chi^{(1)}$ or simply χ) and cubic ($\chi^{(3)}$) susceptibilities of the system in question.

From Eq. (11) it is apparent that in a solid system (immobilized grains) all the susceptibilities depend upon the implemented distribution of anisotropy axes. Let us consider some limiting cases.

Longitudinal alignment: $\boldsymbol{n}\|\boldsymbol{h}$. All the angular functions $P_l(\boldsymbol{nh})$ turn into unity. From Eq. (11) one gets for the susceptibilities

$$\chi_\parallel = \frac{c\mu^2}{k_BT}\frac{1+2S_2}{3}, \quad \chi_\parallel^{(3)} = -\frac{c\mu^4}{k^3T^3}\frac{7+70S_2^2+40S_2-12S_4}{315}. \tag{13}$$

Transversal alignment: $\boldsymbol{n}\perp\boldsymbol{h}$. The angular functions turn into $P_2(\boldsymbol{nh}) = -\frac{1}{2}$ and $P_4(\boldsymbol{nh}) = \frac{3}{8}$ that yields

$$\chi_\perp = \frac{c\mu^2}{k_BT}\frac{1-S_2}{3}, \quad \chi_\perp^{(3)} = -\frac{c\mu^4}{k^3T^3}\frac{14+35S_2^2-40S_2-9S_4}{630}. \tag{14}$$

Random orientation: angular averaging shows that $P_2(\tilde{\boldsymbol{n}}\boldsymbol{h}) = P_4(\tilde{\boldsymbol{n}}\boldsymbol{h}) = 0$ and $[P_2(\tilde{\boldsymbol{n}}\boldsymbol{h})]^2 = \frac{1}{5}$ that results in

$$\tilde{\chi} = \frac{c\mu^2}{3k_BT}, \quad \tilde{\chi}^{(3)} = -\frac{c\mu^4}{k^3T^3}\frac{1+2S_2^2}{45}. \tag{15}$$

Note that we use a tilde to mark the random-orientation averages saving the customary overline for the future to designate size averaging.

From Eqs. (13)–(15) one finds that the linear part of the random-system susceptibility obeys a superposition rule $\tilde{\chi} = [\chi_{\parallel}+2\chi_{\perp}]/3$. Due to that the particle anisotropy falls out of the result. However, the cubic susceptibility turns out to be rather sensitive to it. Indeed, according to Eq. (15) for an assembly of magnetically rigid grains ($S_2 \to 1$) it is three times greater than that of an isotropic ($S_2=0$) system.

Let us compare the formulas for a solid random system with those for an assembly of orientationally free grains, e.g., a magnetic suspension. In the latter case, the extension of the configurational space in the single-particle partition function, i.e., adding integration over $\boldsymbol{n}$ in Eq. (2), removes the effect of the internal anisotropy on the macroscopic magnetization. This results (see Ref. 6, for example) in an isotropic (Langevin) equilibrium magnetization curve that expands yielding

$$\chi_0=\frac{c\mu^2}{3k_BT}, \quad \chi_0^{(3)}=-\frac{c\mu^4}{45k^3T^3}, \tag{16}$$

cf. Eq. (15). Coinciding in linear parts—a fact that has been remarked in Ref. 1—the susceptibilities of a fluid and random solid assemblies differ in the cubic contributions unless one deals with magnetically isotropic particles for which $S_l=0$. This important fact has been overlooked in Refs. 4,5, where the authors have taken Eq. (16) as a starting point to study a solid system. Right from the comparison of the static formulas (15) and (16) for $\chi^{(3)}$ the occurrence of too small predicted values, when Eqs. (16) are used, becomes apparent.

II. DYNAMIC SUSCEPTIBILITIES. GENERAL SCHEME

The rotary diffusion (Fokker-Planck) equation for the distribution function $W(\boldsymbol{e},t)$ of the unit vector of the particle magnetic moment derived by Brown,[7] may be written[8] as

$$2\tau_D\partial W/\partial t=\hat{\boldsymbol{J}}W\hat{\boldsymbol{J}}(U/k_BT+\ln W), \tag{17}$$

where $\hat{\boldsymbol{J}}$ is the operator of infinitesimal rotations with respect to the components of $\boldsymbol{e}$, and $\tau_D \propto T^{-1}$ is the reference time of the internal rotary diffusion of the particle magnetic moment. If the basic dynamics of the latter is described by the phenomenological Landau-Lifshitz equation, then the diffusion time has a simple representation[8]

$$\tau_D=\sigma\tau_0, \tag{18}$$

where τ_0 is the relaxation time of the Larmor precession and is assumed to be temperature independent. Below we make use of the relationship (18) when it becomes necessary to single out temperature dependences.

In the case of isotropic magnetic particles, that is $U=-\mu(\boldsymbol{eH})$, both linear and cubic dynamic susceptibilities may be obtained analytically. To show that, first, we transform Eq. (17) into an infinite set of differential recurrence relations

$$\frac{2\tau_D}{l(l+1)}\frac{d}{dt}\langle P_l\rangle+\langle P_l\rangle-\frac{\xi}{2l+1}(\langle P_{l-1}\rangle-\langle P_{l+1}\rangle)=0. \tag{19}$$

In absence of the external field ($\xi=0$, zero-order solution) the magnetic moments are distributed at random, and

$$P_0=1, \quad \langle P_l\rangle=0 \quad \text{for } l>0. \tag{20}$$

We assume the applied probing field to change harmonically

$$H=\tfrac{1}{2}H_0(e^{i\omega t}+e^{-i\omega t}). \tag{21}$$

Substituting it as $\xi=\mu H/k_BT$ in Eqs. (17), one arrives at a problem that is nonlinear with respect to the field amplitude. However, the field being a probing one, ensures the smallness of ξ, and it allows us to build up a perturbation approach, taking Eq. (20) as the initial step. On doing so, the result obtained in the first order in ξ is

$$M^{(1)}/c\mu=\langle P_1\rangle^{(1)}=\tfrac{1}{6}\xi\left(\frac{e^{i\omega t}}{1+i\omega\tau_D}+\frac{e^{-i\omega t}}{1-i\omega\tau_D}\right).$$

The second-order correction, due to the parity conditions, does not contribute to magnetization, whereas the third order leads to

$$M^{(3)}/c\mu=\langle P_1\rangle^{(3)}=-\frac{\xi^3}{360}\left[\frac{e^{3i\omega t}}{(1+i\omega\tau_D)(1+\frac{2}{3}i\omega\tau_D)(1+3i\omega\tau_D)}+\text{c.c.}\right]-\frac{\xi^3}{360(1+\omega^2\tau_D^2)}$$
$$\times\left[\frac{(3+\frac{7}{3}i\omega\tau_D)e^{i\omega t}}{(1+i\omega\tau_D)(1+\frac{2}{3}i\omega\tau_D)}+\text{c.c.}\right], \tag{22}$$

where c.c. stands for complex conjugates. From Eq. (22) it follows that with respect to frequency the cubic term comprises two harmonics. One oscillates with the single frequency ω and hence yields just a small correction to the linear contribution whereas the other entirely determines the response at 3ω. The corresponding complex susceptibility reads

$$\chi_{3\omega}^{(3)}=\frac{1}{4}\chi_0^{(3)}\frac{1}{(1+i\omega\tau_D)(1+\frac{2}{3}i\omega\tau_D)(1+3i\omega\tau_D)}, \tag{23}$$

where $\chi_0^{(3)}$ is the static value given by Eq. (16).

Formulas like Eqs. (19)–(23) are well known in the theory of rotary molecular diffusion in dipolar fluids, see

Ref. 9, for example. Here we recall their magnetic analogs in order to clarify the difference between our theory and the approach recently developed in Refs. 4,5. The authors of the latter, driven by the intention to extend the superparamagnetic blocking model to a nonlinear case, have done that in the following intuitive way. They simply replaced τ_D in Eq. (23) by the Néel asymptotic expression

$$\tau_N = \tau_0 \exp(\sigma) = (\tau_D/\sigma)\exp(\sigma), \tag{24}$$

and took the corresponding form as $\chi^{(3)}$ for a solid system of randomly oriented uniaxial particles.

Even at the same intuitive level, one can put forward some arguments against such a combination. At least two of them are obvious. First, Eq. (23) with τ_N from Eq. (24) yields an incorrect value for the static ($\omega \to 0$) susceptibiity, cf. Eq. (15). Second, it ignores the fact that the magnetic anisotropy directly imparts the exponential mode only in relaxation of $\langle P_1 \rangle$ leaving the quadrupole one ($\langle P_2 \rangle$) unchanged.

This does not mean, however, that the intuitive way is completely impossible. For example, the approximate form

$$\chi^{(3)}_{3\omega} = -\frac{1}{4}\chi^{(3)}_0 \frac{1+2S_2^2}{(1+i\omega\tau_N)(1+\frac{2}{3}i\omega\tau_D)(1+3i\omega\tau_N)}, \tag{25}$$

is free of the aforementioned qualitative drawbacks and because of that, in principle, has much more grounds to be called a blocking model approximation for $\chi^{(3)}$ than the one of Refs. 4,5. In below we show that Eq. (25) is rather close to the approximation (44) which we consider to be the best.

Resuming the main line of our consideration, now we shall show how to consistently take into account the effect of the particle magnetic anisotropy by solving the Brown equation (17).

Choosing spherical coordinates for the unit vectors $\boldsymbol{e}$, $\boldsymbol{n}$, $\boldsymbol{h}$ as (θ,φ), $(0,0)$, $(\psi,0)$, respectively, i.e., taking $\boldsymbol{n}$ as the polar axis of the framework, one has

$$(\boldsymbol{eh}) = \cos\psi\cos\theta + \sin\psi\sin\theta\cos\varphi, \tag{26}$$

and Eq. (1) may be rewritten as

$$U = -Kv\cos^2\theta - \mu H(\cos\psi\cos\theta + \sin\psi\sin\theta\cos\varphi), \tag{27}$$

The nonstationary solution of the kinetic equation (17) is sought in the form of a spherical harmonics expansion

$$W(\theta,\varphi,t) = \sum_{l=0}^{\infty}\sum_{m=-l}^{l} b_{l,m}(t)\sqrt{\frac{2l+1}{4\pi}\frac{(l-|m|)!}{(l+|m|)!}}Y^*_{lm},$$

$$Y_{lm}(\theta,\varphi) = \sqrt{\frac{2l+1}{4\pi}\frac{(l-|m|)!}{(l+|m|)!}}P_l^m e^{im\varphi}, \tag{28}$$

where the variables are separated and the time dependence is determined by the functions

$$b_{l,m}(t) = \langle P_l^m(\cos\theta)e^{im\varphi}\rangle. \tag{29}$$

The set of complex coefficients $b_{l,m}$ may be found by solving numerically an infinite set of differential recurrence relations obtained by substitution of expansion (28) into Eq. (17):

$$2\tau_D\frac{d}{dt}b_{l,m} + l(l+1)b_{l,m} - 2\sigma\left[\frac{(l+1)(l+m-1)(l+m)}{(2l-1)(2l+1)}b_{l-2,m} + \frac{l(l+1)-3m^2}{(2l-1)(2l+3)}b_{l,m} - \frac{l(l-m+2)(l-m+1)}{(2l+1)(2l+3)}b_{l+2,m}\right]$$
$$-\frac{\xi\cos\psi}{2l+1}[(l+1)(l+m)b_{l-1,m} - l(l-m+1)b_{l+1,m}] - \frac{\xi\sin\psi}{2(2l+1)}[(l+1)(l+m-1)(l+m)b_{l-1,m-1}$$
$$+ l(l-m+2)(l-m+1)b_{l+1,m-1} - (l+1)b_{l-1,m+1} - lb_{l+1,m+1}] = 0. \tag{30}$$

These equations are valid for $m \geqslant 1$. One does not need to consider the negative values of m because of the symmetry of Eq. (28) with respect to the replacement $m \to -m$ that yields $b_{l,-m} = b_{l,m}$. The case $m = 0$ is somewhat special, and the corresponding equation closing the set (28), is to be derived separately. On doing so, it reads

$$2\tau_D\frac{d}{dt}b_{l,0} + l(l+1)b_{l,0} - 2\sigma\left[\frac{(l-1)l(l+1)}{(2l-1)(2l+1)}b_{l-2,0} + \frac{l(l+1)}{(2l-1)(2l+3)}b_{l,0} - \frac{l(l+1)(l+2)}{(2l+1)(2l+3)}b_{l+2,0}\right]$$
$$-\frac{\xi\cos\psi}{2l+1}l(l+1)(b_{l-1,0} - b_{l+1,0}) + \frac{\xi\sin\psi}{2l+1}[(l+1)b_{l-1,1} + lb_{l+1,1}] = 0. \tag{31}$$

We remark that the kinetic equation (17) with the energy function (1) since the pioneering work by Brown[7] has been studied extensively[10,8,11]. However, due to mathematical difficulties the case of arbitrary orientation of the external and anisotropy fields, i.e., vectors $\boldsymbol{h}$ and $\boldsymbol{n}$, has been addressed just recently. The authors of Ref. 12 carried out a numerical solution of the relaxation problem for $\boldsymbol{h}$ and $\boldsymbol{n}$ crossed under an arbitrary angle.

According to this approach, the observed magnetization induced by an external field is found by averaging of Eq. (26) over the distribution function (28) and reads

$$M/c\mu = \langle(\boldsymbol{eh})\rangle = b_{10}\cos\psi + b_{1,1}\sin\psi. \tag{32}$$

The recurrence relations (30),(31) are convenient for constructing a perturbative calculational scheme. Namely, we rewrite Eqs. (30),(31) in a matrix form as

$$2\tau_D \frac{\partial b_{l,m}^{(k)}}{\partial t} + \hat{\Lambda}_{l,l'}^{m} b_{l',m}^{(k)} = \xi e^{\pm i\omega t}[\hat{V}_{l,l'}^{m,m} b_{l',m}^{(k-1)} \cos\psi + (\hat{V}_{l,l'}^{m,m+1} b_{l',m+1}^{(k-1)} + \hat{V}_{l,l'}^{m,m-1} b_{l',m-1}^{(k-1)}) \sin\psi], \tag{33}$$

where $\hat{\Lambda}^m$ is the relaxational matrix for the basic state, and $\hat{V}_{l,l'}^{m,m'}$ are the matrix elements of the perturbation operator, and sums over repeated indices are implicit. This notation explicitly separates the contributions with different m indices in each order of the perturbation procedure. That means that the solution of Eq. (33) may be constructed as a linear combination of the particular solutions of the tridiagonal in index l inhomogeneous equations

$$2\tau_D \frac{\partial a_{l,m}^{(k)}}{\partial t} + \hat{\Lambda}_{l,l'}^{m} a_{l',m}^{(k)} = \hat{V}_{l,l'}^{m,m'} a_{l',m'}^{(k-1)} e^{\pm i\omega t}, \qquad m' = m, m+1, m-1. \tag{34}$$

They could be solved using the continued-fraction method with any desired accuracy.[13] In this sense we call those solutions *numerically exact*.

To distinguish the obtained solutions of Eq. (34) we use the following convention. Let $a_{l,m_1 \ldots m_{j-1}}$ be the value obtained in the preceding iteration. At the present step it enters the right-hand side of Eq. (33) as a perturbation. Then the solution of the current iteration will be designated as $a_{l,m_1 \ldots m_{j-1} m_j}$, that is we simply add the current value of m alongside the second index of a. In this way it is easy to trace back the iteration sequence and recover a correct angular dependence in the final formulas for b_l. As one can see from Eq. (33), every time when the added number differs from its left neighbor, the corresponding contribution to b_l emerges bearing $\sin\psi$ as a factor, otherwise it will bear $\cos\psi$.

III. DYNAMIC SUSCEPTIBILITIES: LINEAR AND CUBIC TERMS

To be able to obtain cubic susceptibilities, the above-described sequence of calculations must be carried out down to the third order.

Zeroth order. Only even harmonics of the distribution function work, and they yield the static contributions

$$b_{l,0}^{(0)} = a_{l,0} = S_l(\sigma),$$

[cf. Eq. (9)] governed by the dimensionless parameter σ, see Eq. (3).

First order. The linear contributions take the form

$$b_{l,0}^{(\omega)} = \tfrac{1}{2}\xi \cos\psi (a_{l,00} e^{i\omega t} + \text{c.c.}),$$

$$b_{l,1}^{(\omega)} = \tfrac{1}{2}\xi \sin\psi (a_{l,01} e^{i\omega t} + \text{c.c.}).$$

Using Eq. (32) one gets the linear complex susceptibility as

$$\chi = \chi_0 (a_{1,00}\cos^2\psi + a_{1,01}\sin^2\psi). \tag{35}$$

The frequency dependence of the linear susceptibility (35) is determined by a superposition of the Debye relaxation modes as

$$a_{1,0m} = \sum_{k=1}^{\infty} \frac{w_k^{(m)}}{1 + i\omega\tau_{k,m}}. \tag{36}$$

The relaxation spectrum of operator $\hat{\Lambda}$ is known to a sufficiently good detail. It consists of one interwell mode τ_{10} becoming exponential in σ at $\sigma \gg 1$ and of an infinite number of intrawell modes $\tau_{1,m}$ with weak σ dependence. As we have recently shown,[14,15] in superparamagnets with a rather good accuracy one may set

$$a_{1,00} = \frac{1+2S_2}{3}\frac{1}{1+i\omega\tau_{10}}, \quad a_{1,01} = \frac{1-S_2}{3}\frac{1}{1+i\omega\tau_{1,1}}. \tag{37}$$

In Eq. (37) the relaxation times are either evaluated numerically or taken in the form of approximate expressions

$$\tau_{10} = \tau_D (1+\sigma/4)^{-5/2} \exp(\sigma), \quad \tau_{11} = 2\tau_D \frac{1-S_2}{2+S_2}. \tag{38}$$

These compact convenient forms were proposed in Refs. 16 and 17, respectively. We emphasize that both of the formulas (38) are *interpolations*, not just asymptotics. As such, they are valid globally, i.e., for the entire range of the parameter $\sigma = Kv/k_BT$. This circumstance considerably facilitates all the approximate calculations.

For a system with randomly oriented anisotropy axes Eq. (35) yields

$$\tilde{\chi} = \chi_0 A_\omega, \quad A_\omega(\sigma, \omega\tau_0) = \tfrac{1}{3}(a_{1,00} + 2a_{1,01}), \tag{39}$$

where A_ω may be called a dispersion factor for the linear susceptibility.

The description rendered by Eqs. (34)–(38) is much more general than the commonly known superparamagnetic blocking model. Indeed, to recover the latter, two limiting transitions are to be done. First, one sets $\omega\tau_D \ll 1$. This assumption is not that strong since this condition on frequency usually holds on up to the MHz range. Then one may neglect the frequency dispersion of $a_{1,01}$ in Eq. (37). For a random assembly it gives

$$\tilde{\chi} = \frac{1}{3}\chi_0 \left[\frac{1+2S_2}{1+i\omega\tau_{10}} + 2(1-S_2)\right]. \tag{40}$$

The second transition is the low-temperature/massive-particle limit: $\sigma \gg 1$. With the aid of Eq. (10) and upon plain replacement of τ_{10} by τ_N from Eq. (24) one gets

$$\widetilde{\chi}=\chi_0\frac{1+i\omega\tau_N/\sigma}{1+i\omega\tau_{\rm N}}, \tag{41}$$

that is entirely equivalent to the blocking model expression for the linear dynamic susceptibilty proposed in Ref. 18 [see formulas (6),(7) there] but now all its terms are completely specified.

According to Eqs. (35)–(41), the blocking model is in fact just the low-frequency end of the low-temperature/massive-particle asymptotics of the superparamagnetic theory. However, this approach is still widely used (see Refs. 4,5, for example) as if it were the only theoretical tool to analyze the micromagnetic relaxation. We remark that the thus imparted incorrectness is easy to trace back if one considers a single particle or an assembly of identical particles. But the situation changes when one has to deal with experimental results and perform size averages, i.e., simultaneously superpose calculations for a wide range of σ. In such a case, of which the situation considered in Refs. 4,5 is a direct example, the implanted mistakes are well hidden and may become more harmful.

Second order. The corresponding coefficients of the expansion (28) write

$$b_{l,0}^{(2\omega)}=\tfrac{1}{4}\xi^2[(a_{l,000}\cos^2\psi+a_{l,010}\sin^2\psi)e^{2i\omega t}+\text{c.c.}],$$

$$b_{l,1}^{(2\omega)}=\tfrac{1}{4}\xi^2[(a_{l,011}+a_{l,001})\sin\ \psi,\cos\ \psi e^{2i\omega t}+\text{c.c.}],$$

$$b_{l,2}^{(2\omega)}=\tfrac{1}{4}\xi^2[a_{l,012}\sin^2\psi e^{2i\omega t}+\text{c.c.}].$$

Though they do not directly affect magnetization, one needs them to proceed to the next order.

Third order. With the ξ^3 accuracy one gets

$$b_{l,0}^{(3\omega)}=\tfrac{1}{8}\xi^3\{[a_{l,0000}\cos^3\psi+(a_{l,0100}+a_{l,0110}+a_{l,0010})\sin^2\psi\ \cos\psi]e^{3i\omega t}+\text{c.c.}\},$$

$$b_{l,1}^{(3\omega)}=\tfrac{1}{8}\xi^3\{[(a_{l,0111}+a_{l,0011}+a_{l,0001})\sin\ \psi\ \cos^2\psi+(a_{l,0101}+a_{l,0121})\sin^3\ \psi]e^{3i\omega t}+\text{c.c.}\}.$$

Using that, for the cubic contribution to the dynamic susceptibility at the triple frequency we find

$$X_{3\omega}^{(3)}=\frac{c\mu^4}{4k_B^3T^3}A_{3\omega},$$

$$A_{3\omega}(\psi,\sigma,\omega\tau_0)=a_{1,0000}\cos^4\psi+(a_{1,0100}+a_{1,0110}+a_{1,0010}+a_{1,0111}+a_{1,0011}+a_{1,0001})\sin^2\psi\ \cos^2\psi+(a_{1,0101}+a_{1,0121})\sin^4\psi. \tag{42}$$

For a randomly oriented assembly one gets

$$\widetilde{X}_{3\omega}^{(3)}=\frac{c\mu^4}{4k_B^3T^3}\widetilde{A}_{3\omega},$$

$$\widetilde{A}_{3\omega}(\sigma,\omega\tau_0)=\tfrac{1}{5}a_{1,0000}+\tfrac{2}{15}(a_{1,0100}+a_{1,0110}+a_{1,0010}+a_{1,0111}+a_{1,0011}+a_{1,0001})+\tfrac{8}{15}(a_{1,0101}+a_{1,0121}). \tag{43}$$

The modes a_1 contributing to $A_{3\omega}$ differ in symmetry and, due to that, in the type of dependence on the dimensionless parameters σ and $\omega\tau_0$. Only for an isotropic case ($\sigma\to0$) all of them have the same high-frequency dispersion (23). As the interwell potential barrier grows ($\sigma\gtrsim1$), the dispersion of the modes whose subscripts have zeroes in even positions, rapidly shifts to lower frequencies. Those modes describe the interwell transition, and for them the frequency parameter tends to $\omega\tau_{\rm N}$ with the exponential $\tau_{\rm N}$ from Eq. (24). For the modes of the ''intrawell origin'' the frequency parameter tends to $\omega\tau_0$ and thus remains in the high-frequency range. As in the linear susceptibility case, the amplitudes of the transverse modes (the last digit in the subscript is 1) vanish with σ whereas those of the longitudinal modes saturate at some finite values.

One may surmise that the low-frequency limit, introduced while discussing the linear relaxation, would simplify the nonlinear case as well since the process is mainly governed by the relaxation time τ_{10}. Indeed, we have found that the approximate expression

$$\widetilde{\chi}_{3\omega}^{(3)}=\frac{1}{4}\chi_0^{(3)}\frac{(1+2S_2^2)(1-i\omega\tau_{10})}{(1+i\omega\tau_{10})(1+3i\omega\tau_{10})}, \tag{44}$$

describes fairly well the frequency dependence of $\chi^{(3)}$ in a randomly oriented assembly.

Formula (44) is simple and easy to use for estimations and calculations. At the same time, we remark that it has been obtained by a heuristic improvement of Eq. (23) in its low-frequency ($\omega\tau_D<1$) form (25) and as such does not have any rigorous justification. Our claim of its quantitative reliability is based on many comparisons done against the numerically exact results.

The results of numerically exact calculations of the dynamic nonlinear susceptibilities for a random assembly of monodisperse grains along formulas (32)–(43) are presented in Figs. 1. We show them as the functions of the temperature parameter $\sigma\propto1/T$, taking the reference value $\omega\tau_0=10^{-8}$ for definiteness. This choice seems reasonable since the low-frequency magnetic measurements are typically carried out at ω about 10^2-10^3 Hz, and the customary reference value of τ_0 is believed to be in the $10^{-10}-10^{-9}$s range. The curves obtained by the approximate formula (44) are plotted with thin dashed lines which visually almost coincide with the curves corresponding to the exact solution.

For comparison in the same figures we present the results of the theory proposed in Refs. 4,5. We remind that this approach suffers from two main drawbacks. First, the authors neglect the dependence of the static susceptibilities on the internal order parameter S_2 introduced by our Eq. (9). Second, they define the frequency dispersion of the cubic term χ_2 taking formula (23)—which is really valid only for the case of isotropic particles—and ''manually'' replacing there the Debye relaxation time τ_D by the Néel asymptotical one $\tau_{\rm N}$ given by Eq. (24).

From Figs. 1 the consequences are apparent. Resembling the exact results in general, the cubic susceptibilities by the theory of Refs. 4,5 display considerable quantitative deviations. In particular, the relative heights of the extrema are

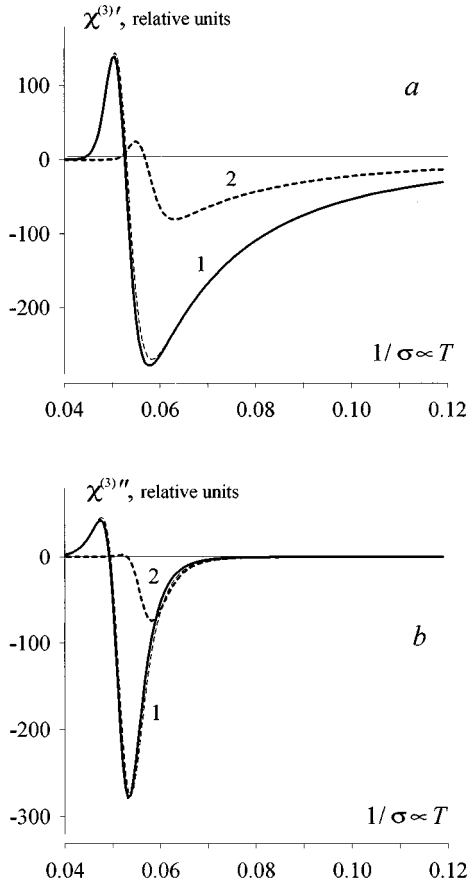

FIG. 1. Real (a) and imaginary (b) part of the cubic susceptibility for $\omega\tau_0=10^{-8}$. *1* indicates the numerically exact solution, *2* is according to the theory by Refs. 4,5; dashed line is approximation (44). Actual numbers on vertical axes render the corresponding χ's divided by coefficient C_3 introduced in Eq. (53)

much smaller that those rendered by the exact solution. Also, the nodes of the curves are considerably shifted along the temperature axis.

IV. MONODISPERSE ASSEMBLIES

The set of formulas derived in the preceding section is self-sufficient for a numerically exact evaluation of the linear and cubic magnetic responses as soon as the material parameters are known. Here we assume that the system is dilute enough and interparticle interaction may be neglected. In this framework, to construct the dependences to be compared to the experimental data, one, first, has to calculate the responses for a subsystem of identical grains with a volume v, and then perform the averaging with an appropriate volume-distribution function $f(v)$.

However, before doing that, it is useful to understand qualitatively the anticipated behavior of the susceptibilities. Let us consider the Debye-type expression Eq. (40) for the linear susceptibility. The drastic change of the exponential factor reduces all the limiting behavior to just two cases. The first is $\omega\tau_{10}\gg 1$, i.e., the system is rather ''cold and stiff.'' Due to that the response is close to zero. The second case is $\omega\tau_{10}\ll 1$. The system is ''warm and soft,'' and readily responds to a signal of almost any frequency.

Estimating on this basis the frequency dependence of the susceptibility (ω grows from zero at given finite T) we conclude on a stepwise change of the real part, $\chi'(\omega)$, and a peak at the imaginary component $\chi''(\omega)$. For both curves the characteristic points are determined by the same condition $\omega\tau_{10}\approx 1$.

The temperature behavior of the said quantities is as easy to foresee. One has just to note that the temperature growth at given frequency is roughly equivalent to reducing of ω in formula (41). The main difference is that the static susceptibility entering Eq. (41) imposes the Curie law $\chi_0\propto 1/T$ [see Eq. (15)] on either curve in the high-temperature range. Therefore, both $\chi'(T)$ and $\chi''(T)$ are expected to have similar contours, be positive and display a peak at a temperature corresponding to $\omega\tau_{10}\approx 1$.

A qualitative behavior of the cubic susceptibility $\chi^{(3)}_{3\omega}$ may be analyzed with the aid of Eq. (44). Separating there the real and imaginary parts, one gets

$$\frac{\chi^{(3)\prime}}{|\widetilde{\chi}^{(3)}_0|}=\frac{7\omega^2\tau_{10}^2-1}{4(1+\omega^2\tau_{10}^2)(1+9\omega^2\tau_{10}^2)},$$

$$\frac{\chi^{(3)\prime\prime}}{|\widetilde{\chi}^{(3)}_0|}=\frac{\omega\tau_{10}(3\omega^2\tau_{10}^2-5)}{4(1+\omega^2\tau_{10}^2)(1+9\omega^2\tau_{10}^2)}, \qquad (45)$$

where $\widetilde{\chi}^{(3)}_0$ stands for the static cubic susceptibility of a random assembly introduced by Eq. (15).

According to Eq. (45), the nonlinear susceptibilities may invert their signs with both frequency and temperature at some points in the $\omega\tau\sim 1$ range. This change is from negative to positive with the frequency growth, and to the contrary with the temperature increase. A simple calculation proves that on the temperature dependences the node of $\chi^{(3)\prime}$ always resides at higher T than that of $\chi^{(3)\prime\prime}$.

To completely clarify the effect of anisotropy on susceptibility of a random assembly, we plot the surfaces in Figs. 2,3. Taking cross sections along the frequency axes, one may observe how the susceptibility curves transform under the anisotropy ($\sigma\propto K$) increase. The isolines $\chi=$const drawn in the underlying planes help to understand the limiting behavior. In the low anisotropy range (here it is $\sigma\lesssim 5$) the ''exponentiality'' of the relaxation time is not pronounced. This produces in each plot short parts of isolines parallel to the σ axes. Further, there occurs a narrow crossover range. After it all the other relaxation modes become insignificant, and the isolines turn into linear dependences $\sigma\propto-\ln\omega\tau_0$. For a given ω, this reflects the growth of the reference relaxation time with σ. Accordingly, in all the plots the parts of characteristic (abrupt) changes of $\chi(\omega)$ move to smaller frequencies approximately logarithmically. Note that since $\sigma\propto 1/T$, cross sections along the σ axes yield the temperature dependences at constant K and frequency.

Some complicated details—inflections and inflations of the representing surfaces—occur in the nearest corner of the plots Figs. 2, 3, i.e., at $\omega\tau_0>1$ and $\sigma\sim 1$. This is the range that is beyond the scope of the low-frequency approximation, and much so the blocking model. Those results are available only by numerical evaluation since one has to take into account on equal basis a wide set of relaxation modes, both

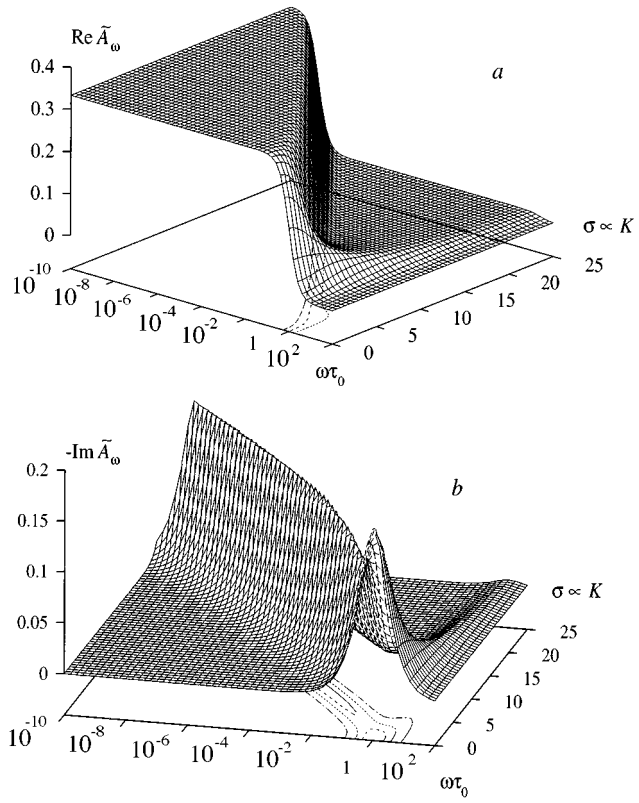

FIG. 2. Monodisperse random assembly. Reduced linear susceptibilty according to Eq. (39) as transformed with the anisotropy growth; *a* is the real part, *b* is the imaginary part.

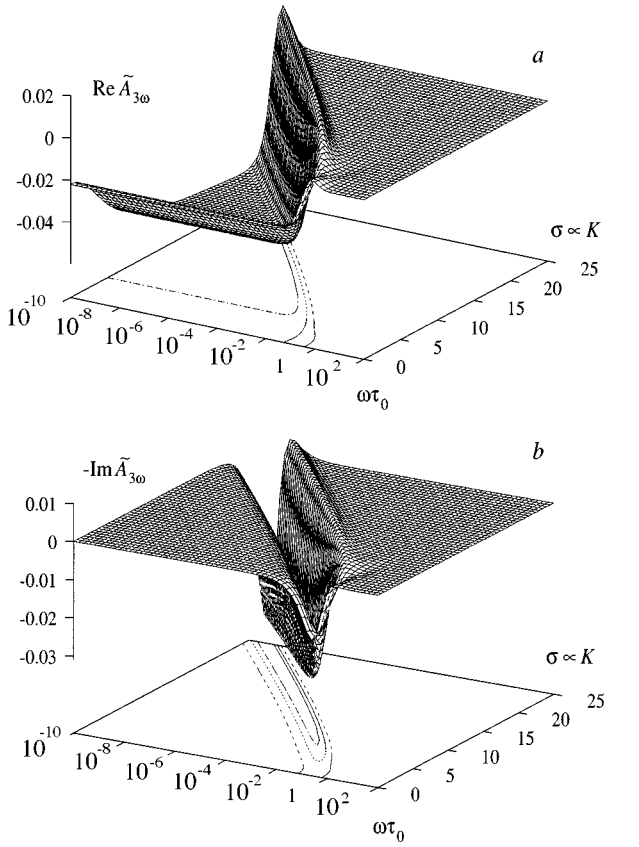

FIG. 3. Monodisperse random assembly. Reduced cubic susceptibilty according to Eq. (43) as transformed with the anisotropy growth; *a* is the real part, *b* is the imaginary part.

transverse and longitudinal. Physically, that means that at those frequencies the intrawell modes yield a noticeable contribution.

The surfaces shown in Figs. 2,3 are interesting as well from the viewpoint that they visualize the theoretical data arrays which are involved when one passes to experiment interpretation. Indeed, performing of size (or volume) averagings of the susceptibilities means superposing of a number of curves each corresponding to its own σ=const cross section with appropriate weights given by the distribution function.

V. POLYDISPERSE SYSTEMS: THE CHOICE OF THE TRIAL DISTRIBUTION FUNCTION

In the majority of cases when one deals with nanosize superparamagnetic grains, polydispersity seems to be an inherent feature. The independent measurement of the size-distribution function, e.g., by electron micrography, is a painstaking and rare opportunity. Besides, even when it is done, from the statistical viewpoint a set of available measurements (10^3-10^4 grains) for the particle number concentration even as small as $10^{10}-10^{12}$, that is 0.01% by volume at the particle size $\sim$10 nm, is far from being statistically representative.

That is why the conventional approach is to choose a trial (model) size-distribution function and determine its parameters upon fitting theoretical curves to the experimental data. By obvious reasons, of the variety of the available distribution formulas, the two-parameter ones are most popular. And of the latter, two are known to work better than others. Namely, they are *the log-normal distribution* given by

$$f_l(v)=\frac{1}{\sqrt{2\pi}sv}\exp\left[-\frac{\ln^2(v/v_{0l})}{2s^2}\right], \tag{46}$$

which is the most famous. Its closeness to real histograms of disperse systems has been reported in thousands of papers. The most probable value v_p of the argument [the position of $f_l(v)$ maximum] and the nth moment are, respectively,

$$v_{pl}=v_{0l},\exp(-s^2), \quad \overline{v_l^n}=v_{0l}^n\ \exp[(ns)^2/2]. \tag{47}$$

The gamma distribution

$$f_g(v)=\frac{1}{\Gamma(\beta+1)v_{0g}}\left(\frac{v}{v_{0g}}\right)^\beta \exp(-v/v_{0l}), \tag{48}$$

where $\Gamma(x)$ is the Euler gamma function. The most probable value v_{pg} and the nth moment are

$$v_{pg}=(\beta+1)v_{0g}, \quad \overline{v_g^n}=(v_{0g})^n\,\frac{\Gamma(\beta+n+1)}{\Gamma(\beta+1)}. \tag{49}$$

The Γ distribution is the generalization of the Poisson one which is also in use, see, for example, Ref. 18. A detailed demonstration of its usefulness for interpretation of the low-frequency magnetic spectra of magnetic fluids (dispersions of nanosize ferroparticles) was given in Ref. 19.

Note, that in given representations (46) and (48) of either of the distribution functions the v_0 parameter is a reference value and does not have a direct meaning of the mean volume. The latter is formed as a particular combination—see Eqs. (47) and (49)—of corresponding v_0 and the distribution width.

When passing to the averaging formulas, one must treat the susceptibility expression like Eq. (41) as yielding a contribution of the jth fraction of the particles with a volume v_j and number concentration c_j. By definition, the latter writes

$$c_j = c(c_j/c) = cf(v)dv, \tag{50}$$

where summation over j is equivalent to integration over v. However, the meaning of c for a polydisperse system is ambiguous, and we replace it by introducing the dimensionless total particle volume fraction

$$\varphi = c\overline{v}. \tag{51}$$

We emphasize that for a polydisperse system replacement Eqs. (50),(51) are the only correct way to eliminate c. Plain substitution of φ instead of cv in formulas (16), as in Refs. 4,5,18, would have been correct only for monodisperse systems.

Let us do that taking Eq. (44) as an example. With the aid of Eqs. (50),(51) it transforms into

$$d\overline{\chi}^{(3)}_{3\omega} = -\frac{\varphi I^4 v^4}{\overline{v}\, k^3 T^3}\widetilde{A}_{3\omega}(\sigma, \omega\tau_0) f(v)dv. \tag{52}$$

It is convenient to scale the current volume as $y = v/v_0$ which does not change the integration limits. Then the current value of the anisotropy parameter becomes $\sigma = (Kv_0/k_BT)y = \sigma_0 y$, and the assembly-averaged cubic susceptibility writes

$$\overline{\chi}^{(3)}_{3\omega} = -C_3\sigma_0^3\frac{v_0}{\overline{v}}\int_0^\infty y^4 f(y)\widetilde{A}_{3\omega}(\sigma_0 y, \omega\tau_0)dy,$$

$$C_3 = \varphi I^4/K^3. \tag{53}$$

Similarly, for the linear susceptibility one gets

$$\overline{\chi} = C_1\sigma_0\frac{v_0}{\overline{v}}\int_0^\infty y^2 f(y)\widetilde{A}_{\omega}(\sigma_0 y, \omega\tau_0)dy, \quad C_1 = \varphi I^2/K, \tag{54}$$

where now the temperature dependence is described by the argument $\sigma_0 \propto 1/T$. Evidently, formulas (53),(54) show the general way of volume averaging for χ and $\chi^{(3)}_{3\omega}$ and hold for the exact dispersion factors A as well as for their approximations.

In Fig. 4 we visualize the averaging procedure described by Eqs. (53),(54). The dispersion factors are evaluated by the numerically exact procedure. The plots show the evolution of the susceptibility curves $\chi'(T)$ with the widening of the lognormal distribution. The front plane $s=0$ corresponds to the monodisperse case $f(v) \propto \delta(v - v_0)$ considered in Fig. 1. Besides the expected smearing down of sharp peaks, from the sequence of the level lines one observes that as the distribution width grows, the positions of the main extrema drift to the higher temperature range. Very qualitatively, this tendency may be understood from the relation $T \propto K\overline{v}/k_B$ where the mean value is determined by Eq. (47). We remark that for a great many of dispersed systems the typical values of s fall into the interval 0.5 ± 0.2.

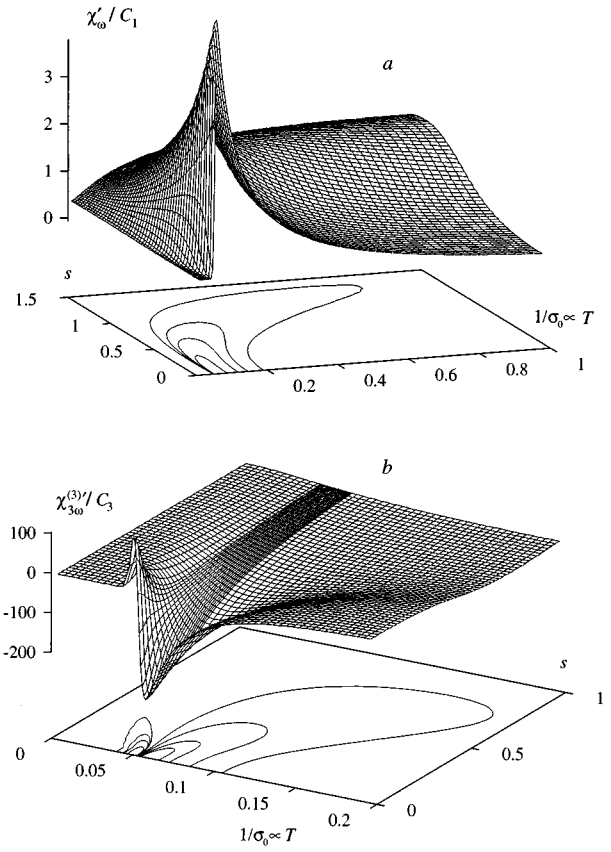

FIG. 4. Modeling of the lognormal volume-averaging effect. Real parts of the linear (a) and cubic (b) susceptibilities for $\omega\tau_0 = 10^{-8}$.

VI. POLYDISPERSE SYSTEMS: COMPARISON WITH EXPERIMENT

For practical comparison we take an ample set of experimental data reported in Ref. 4 (and confirmed in Ref. 5) on linear and cubic susceptibilities of Cu–Co precipitating alloys. The given data cover the frequency domain 30–840 Hz and the temperature range 10–150 K. Synthesis of the samples as well as the method of magnetic measurement are described. However, apart from the observation that Cu–Co alloys precipitate yielding a dispersion of cobalt nanosize particles in a copper matrix, no particular structural information on the system is given.

When the superparamagnetic theory is applied for interpretation of any measured susceptibility line, it means that some model function $\chi(v, \omega, T)$ depending on several material parameters is processed through averaging like Eq. (53) or (54). In our case the basic set of the material parameters comprises magnetization I, anisotropy energy density K, relaxation time τ_0, and the particle volume fraction φ. Obviously, for nanosize-dispersed systems the effective values of I, K, and τ_0 do not coincide with those for a bulk material.

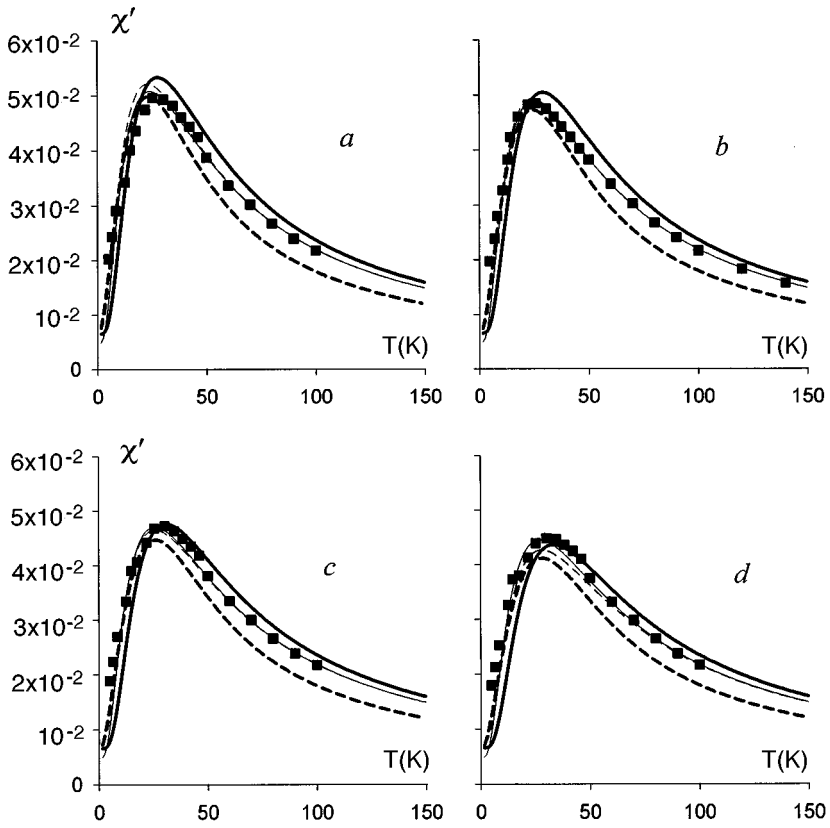

FIG. 5. Linear susceptibility, real part. Comparison with the experiment by Ref. 4 for the frequencies: 30 Hz (a), 80 Hz (b), 220 Hz (c), 840 Hz (d). Volume averaging is performed with the magnetic and statistical parameters according to Table I. Entry 1 indicated by thick solid lines, entry 2 indicated by thick dashed lines, entry 3 indicated by thin solid lines, entry 4 indicated by thin dashed lines. Almost everywhere the two latter visually coincide. The vertical scale coincides with the one adopted in Refs. 4,5 for the experimental data.

The size/volume averaging itself introduces two independent statistical parameters. Therefore, the fitting procedure turns into an optimization problem in a multidimensional parameter space with rather loose restrictions.

Due to that one should not expect that the analysis of just the susceptibility temperature-frequency behavior is self-sufficient for unambiguous determination of the magnetic material parameters. But it is reasonable to ask what is the real extent to which one could reduce the uncertainty while fitting the measured data.

First we remark that in the framework of the proposed theory the number of independent parameters determining the susceptibilities of a superparamagnetic assembly, equals five. Indeed, from Eqs. (53),(54) and (47),(49) it follows that the reference volume as such does not enter the results. It appears just in the combination Kv_0/k_B. Denoting it as T_0, one may rewrite Eqs. (53),(54) as

$$\overline{\chi_{3\omega}^{(3)}} = -C_3\left(\frac{T_0}{T}\right)^3 \cdot \mathcal{A}_3\left(\frac{T_0}{T}, \omega\tau_0, s\right),$$

$$\overline{\chi} = C_1\left(\frac{T_0}{T}\right) \cdot \mathcal{A}_1\left(\frac{T_0}{T}, \omega\tau_0, s\right), \tag{55}$$

(for the Γ distribution, one would have β instead of s). In Eqs. (55) the quantities $\mathcal{A}_1$ and $\mathcal{A}_3$ stand for the integrals of the dispersion factors multiplied by the ratio $v_0/\overline{v}$ which depends solely on the distribution width s or β.

Thus, the set of parameters yielded by fitting comprises T_0, τ_0, s, and two amplitudes C_1 and C_3. From the definitions of the latter—see Eqs. (53),(54)—one sees that they incorporate three material parameters of the system. That means that either I, K or φ may be taken as arbitrary. Note that if one would have dealt with just linear susceptibility measurements, then C_3 does not appear, and the uncertainty of the choice would have been enhanced allowing two of the three parameters as arbitrary. In our case, we set the magnetization of the cobalt particles equal to its bulk value $I=1460$ G. On doing that, one gets explicit relationships

$$v_0 = (k_B/I)\sqrt{C_3/C_1}, \quad K = T_0 I\sqrt{C_1/C_3},$$

$$\varphi = (C_1/I)\sqrt{C_1/C_3}, \tag{56}$$

relating the customary physical parameters to the results of the fitting procedure.

We perform nonlinear fitting using the Levenberg-Marquardt method implemented in the MRQMIN routine.[20] From the experimental end, eight families of data are involved, viz. $\chi'(T)$ and $\chi_{3\omega}^{(3)\prime}(T)$ at four frequencies, taken from Ref. 4. From the theory end, we employ formulas (53)–(56) with the numerically exact dispersion factors. The results of fitting are presented in Figs. 5,6, and in Table I.

VII. DISCUSSION

The fitting process worked sufficiently stably, that means that the set of susceptibilities as a function of its magnetic and statistical parameters does not have too many local minima. So, the sets of values presented in the first two lines of the Table I are unique in a wide vicinity of the parameter space. The results given in Figs. 5,6 have almost equal statistical residuals for the lognormal and gamma functions. However, from the simple *chi-by-eye* viewpoint, the lognormal distribution seems far more satisfactory. For the Γ distribution two flaws are apparent. Namely, noticeable devia-

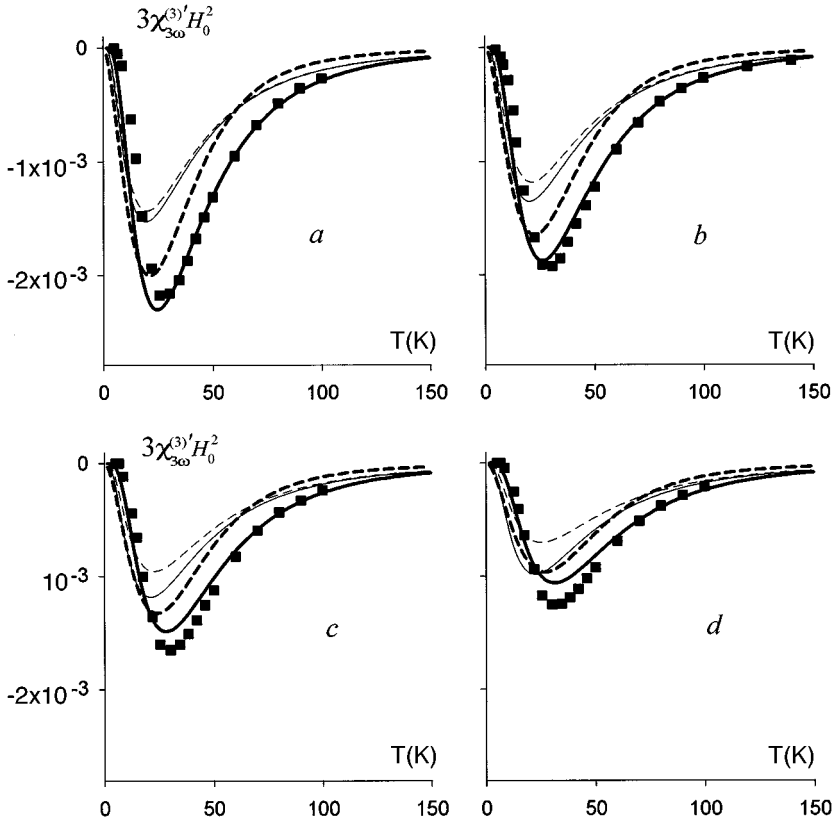

FIG. 6. Cubic susceptibility, real part. Comparison with the experiment by Ref. 4 for the frequencies: 30 Hz (a), 80 Hz (b), 220 Hz (c), 840 Hz (d). The line drawing convention is the same as in Fig. 5. The vertical scale coincides with the one adopted in Refs. 4,5 for the experimental data.

tions at high T and misplacements of the peak positions for both linear and cubic curves.

The main difference between the lognormal and Γ distributions is their reduction rate at the right end, i.e., at $v \to \infty$. As one may see from Eqs. (53),(54), the higher is the susceptibility order the greater is the enhancement of the right-end effect, since under the integral $f(y)$ is multiplied by yet higher powers of y. Apparently, one has no basis to expect that a histogram of a real system would obey any simple two-parameter function. But since χ and $\chi^{(3)}$ are determined by different moments of the distribution, their simultaneous consideration is an effective method to single out the appropriate and inappropriate ones. According to our evidence, for the Co–Cu systems the lognormal distribution is far better.

At the same time, we remark that if to estimate the difference between the two undertaken fittings in terms of statistical moments, the occurring deviations are rather moderate. Indeed, evaluating mean volume and mean-square volume from formulas using the numbers from the Table I (entries 1 and 2), one gets for the lognormal and Γ cases

$$\overline{v_l} = 4.43 \text{ nm}, \quad \sqrt{\overline{v_l^2}} = 4.71 \text{ nm},$$

$$\overline{v_g} = 4.11 \text{ nm}, \quad \sqrt{\overline{v_g^2}} = 4.46 \text{ nm},$$

respectively. Thus one sees that visual comparison happens to be a sensitive test. The differences in Figs. 5,6 are rather pronounced whereas the deviations in mean and mean-square particle diameters do not exceed 8 and 6%, respectively, which is a fairly good accuracy.

It is essential to emphasize, however, that even a very good fitting may be completely misleading unless it matches

TABLE I. Magnetic and statistical parameters obtained by fitting; for all the entries the saturation magnetization is $I = 1460$ G.

	Fitting attempt	Reference relaxation time, sec	Reference volume, cm^3	Standard deviation	Volume fraction, %	Anisotropy constant, erg/cm^3
1	Lognormal, present fit	2.13×10^{-10}	3.79×10^{-20}	0.608	0.704	7.62×10^{5}
2	Gamma, present fit	5.32×10^{-11}	2.30×10^{-20}	$\beta=0.585$	0.738	8.36×10^{5}
3	Lognormal, after Ref. 4	1.60×10^{-14}	5.6×10^{-20}	0.72	0.60	8.8×10^{5}
4	Lognormal, after Ref. 5	1.00×10^{-10}	5.6×10^{-20}	0.72	0.60	5.8×10^{5}

physical considerations. By that we mean that presently there exists enough knowledge on the static and dynamic properties of magnetic nanosize systems to impose a reasonable frame on the orders of magnitude of the sought for parameters. From this viewpoint, the numerical values obtained by fittings with both lognormal and Γ distributions are quite reasonable (entries 1 and 2 in Table I). On the contrary, attempting a quantitative explanation with the aid of a lognormal distribution, the authors of Ref. 4 have obtained some agreement between their theory and experiment setting $\tau_0 \sim 10^{-14}$ s, see the third entry of Table I. The contradiction is apparent: whatever is the *chi-by-eye* agreement in the graphs, the set of parameters should be discarded. The matter is that so short a time is completely forbidden in superparamagnetic particles, see Ref. 21, for example. Probably, just those considerations caused the same authors reinterpret in Ref. 5 their data—see the fourth entry of Table I—with $\tau_0 \sim 10^{-10}$. However, the result of fitting given in Ref. 5—see thin lines in Figs. 5, 6, though rather good for χ', suffers from a serious flaw with respect to $\chi_{3\omega}^{(3)\prime}$. Namely, the position of the theoretical temperature peak is considerably shifted from the experimental one to the low-temperature region. Supposedly, this discrepancy results from the joint effect of using a not completely consistent theory and not too thorough fitting procedure.

In this connection we make note of a fact that we have run into during our own fitting work. As long as we tried the procedure involving just the linear susceptibility data, the best-fit routine, whatever was the initial set, ''stubbornly'' lead us deep into the unphysical region of far too small reference τ's. As soon as the data arrays were extended to include the cubic susceptibilities as well, the best-fit parameter set (entries 1 and 2 of Table I) immediately became reasonable.

CONCLUSIONS

We present a consistent theory of linear and cubic dynamic susceptibilities of a noninteracting superparamagnetic system with uniaxial particle anisotropy. The developed scheme is specified for consideration of the assemblies with random axes distribution but may be easily extended for any other type of the orientational order imposed on the particle anisotropy axes. A proposed simple approximation is shown to be capable of successful replacement of the results of numerically exact calculations.

The theory is tested with the aid of an ample data array on low-frequency magnetic spectra of solid Co–Cu nanoparticle systems. On doing so, we combine it with the two most popular volume distribution functions. When the linear and cubic dynamic susceptibilites are taken into account simultaneously, the fitting procedure yields a unique set of magnetic and statistical parameters and enables us to conclude the best appropriate form of the model distribution function (histogram). For the case under study it is the lognormal distribution.

The achieved agreement yields one more serious argument in favor of the idea that magnetic measurements may work as a sensitive and reliable quantitative material science test for nanosize systems.

Note added in proof

Recently we have tested the approximate susceptibility formulas (40) and (44) using for τ_{10}, instead of Eq. (38), the expression

$$\tau_{10} = \tau_D \frac{e^{\sigma}-1}{2\sigma}\left[\frac{1}{1+1/\sigma}\sqrt{\frac{\sigma}{\pi}}+2^{-\sigma-1}\right]^{-1},$$

proposed by Coffey *et al.* in Ref. 22. As a result, we have to admit that the latter formula indeed realizes a much better approximation to the exact solution than Eq. (38) for both linear and cubic susceptibilities.

Recently, a paper[23] also dealing with nonlinear susceptibilities of fine magnetic particles has appeared. However, the authors of the latter in their consideration address only the equilibrium case. Comparison of the results of Ref. 23 with those of our Sec. I obtained independently, reveals their complete coincidence.

ACKNOWLEDGMENT

This work has been partially supported by RBRF under Grant No. 96–02–16716.

[1] C. P. Bean and J. D. Livingston, J. Appl. Phys. **30**, 120S (1959).
[2] E. Kneller, in *Magnetism and Metallurgy*, edited by A. Berkowitz and E. Kneller (Academic, New York, 1982), Vol. 1. Chap. 8.
[3] A. F. Pshenichnikov, V. V. Mekhonoshin, and A. V. Lebedev, J. Magn. Magn. Mater. **161**, 94 (1996).
[4] T. Bitoh, K. Ohba, M. Takamatsu, T. Shirane, and S. Chikzawa, J. Phys. Soc. Jpn. **64**, 1311 (1995).
[5] S. Chikazawa, T. Bitoh, K. Ohba, M. Takamatsu, and T. Shirane, J. Magn. Magn. Mater. **154**, 59 (1996).
[6] D. A. Krueger, J. Appl. Phys. **50**, 8169 (1979).
[7] W. F. Brown, Jr., Phys. Rev. **130**, 1677 (1963).
[8] Yu. L. Raikher and M. I. Shliomis, Sov. Phys. JETP **40**, 526 (1974); Adv. Chem. Phys. **87**, 595 (1994).
[9] W. Coffey, M. Evans, and P. Grigolini, *Molecular Diffusion and Spectra* (Wiley, New York, 1984).
[10] A. Aharoni, Phys. Rev. **177**, 793 (1969); Phys. Rev. B **7**, 1103 (1973); **46**, 5434 (1992).
[11] W. T. Coffey, D. S. F. Crothers, Yu. P. Kalmykov, E. S. Massawe, and J. T. Waldron, Phys. Rev. E **49**, 1869 (1994); W. T. Coffey, D. S. F. Crothers, Yu. P. Kalmykov, and J. T. Waldron, Phys. Rev. B **51**, 15 947 (1995).
[12] W. T. Coffey, D. S. F. Crothers, J. L. Dormann, L. J. Geoghegan, Yu. P. Kalmykov, J. T. Waldron, and A. W. Wickstead, Phys. Rev. B **52**, 15 951 (1995).
[13] H. Risken, *The Fokker-Planck Equation, Methods of Solutions and Applications* (Springer-Verlag, Berlin, 1989).
[14] Yu. L. Raikher and V. I. Stepanov, J. Phys. Condens. Matter **6**, 4137 (1994).
[15] Yu. L. Raikher and V. I. Stepanov, Europhys. Lett. **32**, 589 (1995).
[16] L. Bessias, L. BenJaffel, and J. L. Dormann, Phys. Rev. B **45** 7805 (1992).
[17] M. I. Shliomis and V. I. Stepanov, J. Magn. Magn. Mater. **122** 176 (1993).

[18] J. I. Gittleman, B. Abeles, and S. Bozowski, Phys. Rev. B **9**, 3891 (1974).
[19] A. F. Pshenichnikov and A. V. Lebedev, Sov. Phys. JETP **68**, 498 (1989).
[20] W. H. Press, B. P. Flannery, S. A. Teukolsky, and W. T. Vetterling, *Numerical Recipes. The Art of Scientific Computing* (Cambridge University Press, Cambridge, 1989).
[21] J. Zhang, C. Boyd, and W. Luo, Phys. Rev. Lett. **77**, 390 (1996).
[22] W. T. Coffey, P. J. Cregg, D. S. F. Crothers, J. T. Waldron, and A. W. Wickstead, J. Magn. Magn. Mater. **131**, L301 (1994).
[23] J. L. García-Palacios and F. J. Lázaro, Phys. Rev. B **55**, 1006 (1997).